Fatigue Properties of 3D Printed Maraging Steel

Nandhini Raju*, and David W. Rosen†

*Department of Mechanical and Aerospace Engineering, University of Central Florida, Orlando, FL 32816.
†Digital Manufacturing and Design Centre, Singapore University of Technology and Design, Singapore 487372.
†School of Mechanical Engineering, Georgia Institute of Technology, Atlanta, GA 30332.

*Corresponding author: nandhini@knights.ucf.edu

Abstract

The objective of this paper is to investigate fatigue properties of maraging steel, in the fabricated, machined, and heat-treated conditions, printed by powder bed fusion. Samples were manufactured in an EOS M280 machine in the X and Z build directions. Manufactured samples were tested under four different conditions: fabricated, machined, heat-treated, and heat-treated and machined. Each condition was expected to have different fatigue properties. The maximum stress and number of cycles to failure results were compared to understand the influence of the different build orientations and conditions on fatigue properties and limits. Results showed that machining and heat treatment, individually and together, had significant effects on fatigue properties. Additionally, the selection of standards, selection of sample counts, and statistical analysis of results will be discussed along with the maraging steel fatigue properties.

Introduction

Additive manufacturing is also known as rapid prototyping or 3D printing. AM techniques have a significant influence over the automotive, aerospace, medical field. Also, it changed the total experience of the manufacturing itself. AM has its unique set of advantages over conventional manufacturing such as less time for manufacturing, being capable to manufacture any complex designs, design freedom, and less material wastage. Due to these advantages, these techniques are getting much attention in industry and academia. Generally, AM techniques can be categorized into seven process categories[1]. Of interest to this paper, metal powder bed fusion (PBF) techniques are used commonly in many industries due to their high density and low porosity end products. However, after melting, the material cools down rapidly, causing high-temperature gradients that leave residual stress in the material and influence the material's strength especially fatigue strength.

Materials such as maraging steels are used in aviation, motor, and military applications due to their high toughness, high ultimate tensile strength along with its high ductility, and weldability[2][3]. Several researchers are working on the mechanical and material properties to improve the strength of the printed steel. Fatigue properties are important for many applications. Generally, a fatigue test is done by applying cyclic loading which is less than the yield strength of the material at static loading. Cyclic loading can be tensile, compressive, or a combination of both. Before material reaches the fracture stage, crack initiation and crack growth are developed in the

material[4]. Crack initiation can happen at the surface or subsurface region due to surface defects such as cracks, porosity, and inclusions. After initiation, a crack grows along the slip plane and is further propagated in the material. This can be predicted in microstructure analysis which can be indicated by striations on the surface [4]. When stress intensity is higher than the material's strength it leads to fracture. Fatigue limit and endurance limit are determined after the collection of stress amplitude and life cycle data, which is typically plotted as the well-known S-N curve. Usually, materials used in an application are subject to loading conditions below the fatigue limit for safety considerations. Usually conventionally manufactured maraging steels' fatigue limit is known as 50% of its UTS (ultimate tensile strength) [5]. But the fatigue limit of maraging steel manufactured by additive manufacturing is 20-30% of its UTS which is much lower than conventionally engineering materials [6]. So, improving the fatigue limit for the additive manufacturing part is important especially for the materials used in harsh environments such as maraging steel.

Maraging steels are known to be precipitation-hardened steels, with intermetallic precipitates forming as the result of aging heat treatments. These precipitates are formed from the various alloying elements, including Fe, Ti, Ni, Al, and Mo, with Ni_3Ti predominating. The aging heat treatment used in this work was performed at 490 °C for 6 hours. Grade 300 maraging steel was used in this study. After aging, ultimate tensile strength increases from around 1100 MPa to 2000 MPa. Hardness improves by a similar amount, while elastic modulus increases by approximately 20 percent.

Literature review

Fatigue testing can be performed with either bending loading or axial loading. The loading cycle can be symmetric, asymmetric, and random type according to stress and time. Usually, ferrous materials such as steel alloys have fatigue and endurance limits, that is finite lives, but non-ferrous alloys such as aluminum alloys may not have endurance limits. Usually, fatigue has three failure modes that consist of crack initiation, propagation, and catastrophic fracture. Generally, shear flow along the slip plane generates the intrusion and extrusion due to the loading cycle. These create surface defects and later it initiates the crack on the surface especially in sharp corners. Tensile loads can fasten crack propagation of the material and compressive stress closes the crack. So tensile load helps to open the crack and compress does the opposite. The repeated loading of tension and compression helps to propagate a crack in the material. Cross-sections of the fatigue failed material can be helpful to predict the propagations. Generally, fatigue tests are influenced by surface cracks, surface roughness, grain size, residual stress, and environment[4].

Material such as maraging steel is high in hardness and it may produce surface cracks easily due to its brittleness. To reduce the number of surface defects, several attempts such as machining, shot peening, surface finishing were usually used. Also, for conventionally engineered maraging steels, different aging treatments enhance the tensile strength, which leads to improved fatigue strength of the material[7]. Also, it is observed that decreasing the aging temperature of conventionally manufactured steels decreased the austenite fraction and interparticle spacing which resulted in improving strength. To improve the fatigue strength different attempts such as changing the chemical composition, nitriding, and shot-peening[8] the manufactured steel were done. Particularly, nitriding the conventional maraging steel increased the fatigue strength due to hardening[9]. As part of hardening, it formed compressive residual stresses in the surface, which

benefits fatigue strength. Different types of fatigue tests have been developed such as the ultrasonic fatigue test, very high cyclic test (VHCF) to understand the limitations of the materials [10]. From these tests, it is observed that inclusions were the origin of crack initiation [11]. Especially inclusions such as Ti-N and aluminate were the main reasons for the crack initiation. Also, even 0.6μm inclusions[12] lead to initial cracks in the surface and sub-surface region which lead to fracture.

According to the authors' knowledge, limited fatigue-related research is available for additively manufactured (AM) maraging steels. Suryawanshi et.al stated that fine cellular structure observed in SLM printed maraging steel showed higher strength when it was aged, and it was comparable with wrought material[2]. Intermetallic components (Fe-Mo based, Ni-based) present within the finer cellular structure were the main reason for the improved ultimate tensile strength, which eventually resulted in improving the fatigue limit of the material. Similar to aging, some researchers have noted that build orientation did affect the fatigue life[13], while other researchers reported that they observed no variation regarding build orientation in fatigue strength[5][14]. Due to the number of variables in PBF processes, using the same build with the same powder, same parameters, etc, was crucial to consolidate the results. Antunes et.al reported the propagation of crack growth in between the layer was significant. This proved the importance of bonding strength and usage of process parameters to manufacture the samples[15]. Sometimes process parameters played an important role to manufacture the quality dense parts. It was reported by Santos et.al that higher scan speeds lead to high porosity[16]. Little is known about the effects of build orientation and post-processing treatments on the fatigue behavior of the EOS MS1 maraging steel material. In this research, build orientation and different post-processing conditions such as-printed, printed and machined, heat-treated, and heat-treated and machined are considered in characterizing the fatigue life of the EOS MS1 material.

Research Methodology

Maraging steel specimens were manufactured by the EOS M280 system using EOS MS1 powder at the Singapore University of Technology and Design. Four different post-processing conditions were examined including as-printed(A), printed and machined (B), heat-treated(C), and heat-treated and machined(D). According to the experimental campaign, samples for each condition were printed in the same build with the same powder to avoid the variance in the results.
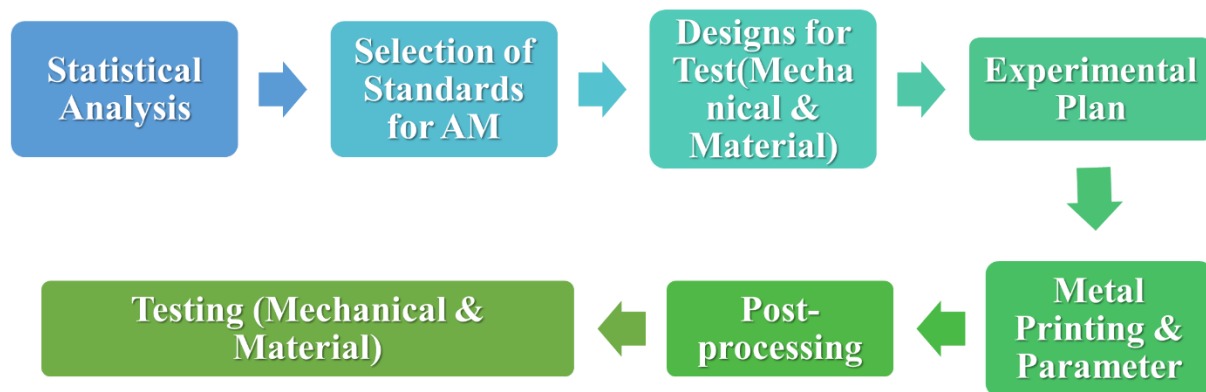
Figure 1 flow chart of the proposed characterization method (reproduced with permission[17])

After the selection of the different post-processing conditions, sample counts are selected based on the characterization method described in the flow chart in Fig.1, which was explained in detail in the authors' previous work[17]. Sample counts were decided to provide a higher confidence interval based on the ASTM E122-17[18] standard and the selection of standards for AM was derived from the NISTIR 8005[19] technical report. Since a limited number of standards are available for AM, finding the equivalent conventional standard for additively manufactured test coupons was important. For the investigation of fatigue properties, the ASTM E0466-15 standard was selected, and design was also observed from the standard.

Based on the statistical method described in the flow chart as well as budget limitations, sample counts were decided as shown in Table 2. For this study direction of the build was considered as another variable. Therefore, X and Z direction samples along with four different post-processing conditions were considered for the experimental campaign to understand the influence on the fatigue properties.

Experimental Plan

Metal printing & parameters:

Generally, maraging steels are low carbon steel with high strength and ductility. In this research EOS MS1 maraging steel powder was used. The chemical composition was derived by combustion-infrared absorbance and is mentioned in Table 1. Also, the particle size of the powder was in the range of 20 microns to 47 microns.

Table 1 Chemical composition of EOS MS1(Reproduced with permission [17])

Ni	Co	Mo	Ti	Al	Cr	Cu	C[a]	Mn	Si	P	S[a]	V	Fe
18.37	9.07	4.97	0.67	0.09	0.18	0.02	0.007	0.04	0.05	<0.01	0.004	0.06	base

Chemical compositions mentioned in weight percentage; [a] -components were determined by combustion-infrared absorbance

As mentioned, maraging steel fatigue samples were manufactured on an EOS M 280 machine. Initially, CAD files were prepared for the X and Z direction build. The preprocessing software for the machine produced the support structures. For this research, the block-type hatch support structure is used. For this research, the "performance" parameter set was selected from the EOS parameter sheet[20].
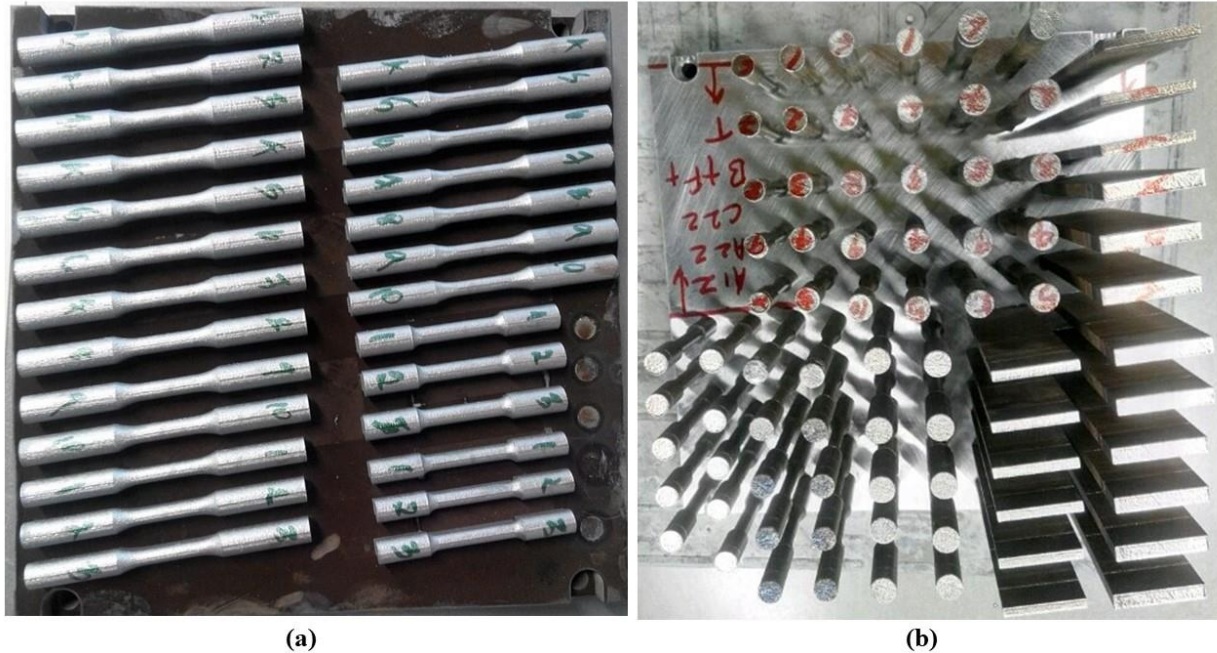

<div align="center">(a)   (b)</div>

Figure 2(a) top view of X-direction printed fatigue samples after the heat treatment (b) top view of Z-direction printed fatigue samples along with other test samples (without heat treatment)

Samples were printed in X, Z direction and shown in Fig.2. Samples were printed for as-printed(A) condition and removed from the build plate by using wire cutting by Electrical Discharge Machining (EDM). For condition B, specimens were designed to be larger than normal so that 1mm of material could be removed from specimen surfaces by turning. These samples were printed, removed from the build plate by wire cutting, and further machined. For condition C, samples were printed from the machine and placed into the furnace before removal from the build plate. Similarly, for condition D, samples were printed, heat-treated, removed from the build plate by wire cutting, and further machined. These four different post-processing conditions were considered for this study and elaborated in Table 2 as an experimental plan.

<div align="center">Table 2 Experimental plan</div>

Direction of build	Printed(A)	Printed & Machined (B)	Heat treated(C)	Heat treated & machined (D)
X	20	20	10	20
Z	20	20	10	20

Fatigue testing

Fatigue specimen geometry was derived from the ASTM E0466-15 standard and mentioned in Fig.3. During the design process, support structure height and wire cutting machine's

wire thickness should be considered to avoid damage to the specimen during the wire cutting. For this research 1mm and more were added to support structure height. Similarly, specimens selected for machined conditions (B, D) had a 1 mm machining (turning) allowance added during design. The selected test method was for axial fatigue loading and especially the high cycle fatigue (HCF) method was followed.
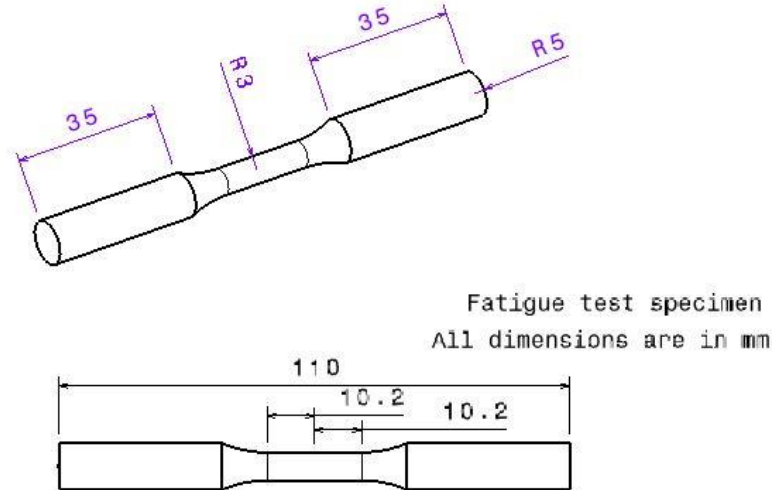

Figure 3 Specimen geometry for fatigue test

Fatigue tests were performed in IMR Test Labs, Singapore. MTS 810(model 318.1), MTS 370(model370.1), Instron 3(model no 8801) frames with different load capacities were used to perform the fatigue testing. For this study, a fully reversed loading cycle was applied. Based on the fully reversed axial loading S-N curve was formed with stress amplitude and number cycles (log scale) in the Y and X-axis.

Results & discussions

For the fatigue test ideally, a large number of test samples is required. An experimental campaign was designed with 10-20 and more samples for each condition. Fatigue tests were performed according to the ASTM standard with reversed cycle conditions. Usually, a fully reversed cycle follows $\sigma_{max}(maximum\ stress\ or\ tensile) = -\sigma_{min}(minimum\ stress\ or\ compressive)$, stress ratio: R=-1, Amplitude ratio: A= infinity. Samples were placed in grips and push-pull axial loads were applied for the fatigue test at room temperature. HCF regime of the test was considered for the analysis.
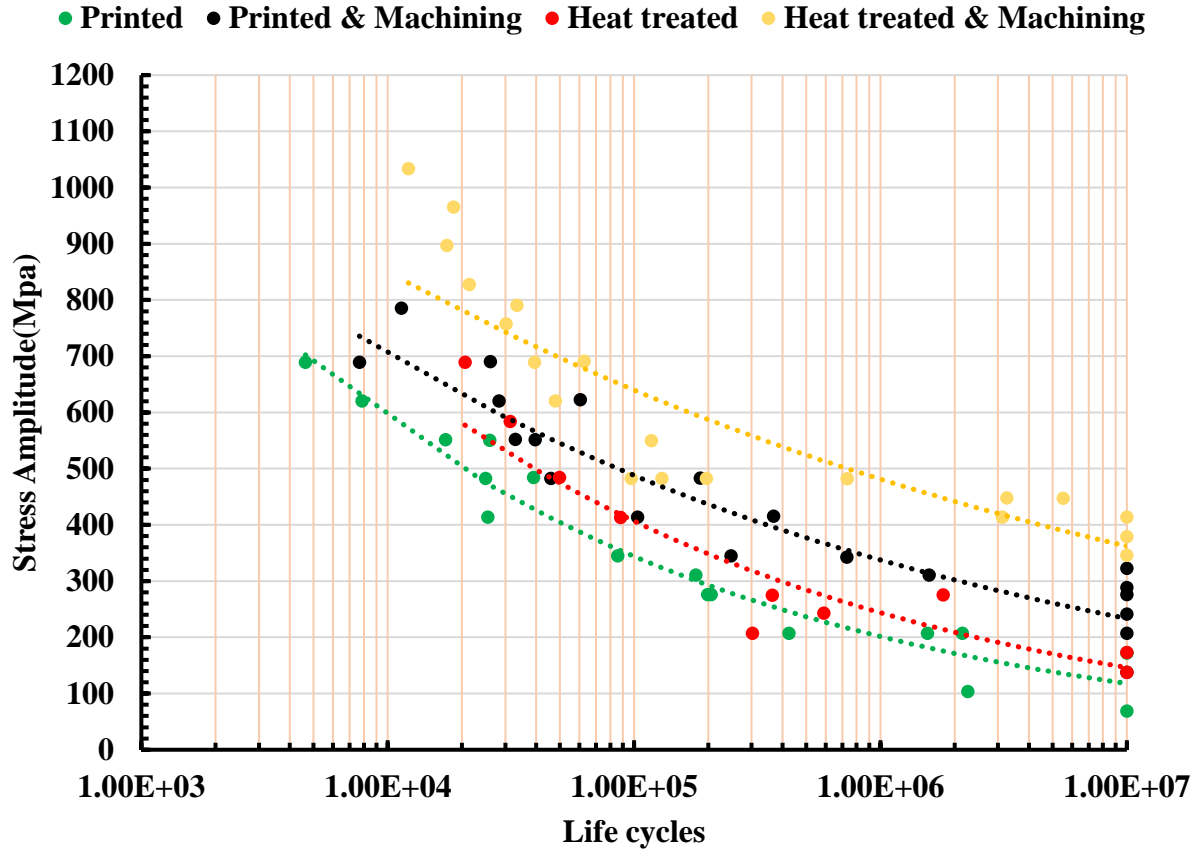
Figure 4 S-N curves for the samples printed in the X-direction.

Since it was an HCF test, the "Stress-lifecycle (S-N) approach" fatigue failure model was used for this study. But using this method, distinguishing crack initiation and propagations was difficult. To define further about S-N approach, the equations listed below were utilized in this research.

$$cyclic\ stress\ range: \Delta\sigma = \sigma_{max} - \sigma_{min} - - -Equation\ 1$$

$$Stress\ amplitude: \sigma_a = \frac{\sigma_{max} - \sigma_{min}}{2} - - -Equation\ 2$$

$$Mean\ stress: \sigma_m = \frac{(\sigma_{max} + \sigma_{min})}{2} - - -Equation\ 3$$

$$Stress\ ratio: R = \frac{\sigma_{min}}{\sigma_{max}} - - -Equation\ 4$$

$$Amplitude: A = \frac{\sigma_a}{\sigma_m} - - -Equation\ 5$$

σ_{max} is different for each post-processing condition's fatigue test. Also, the cyclic stress range for the fatigue test was reduced to understand the life cycle of the material. Once the fatigue test was performed in the MTS machines, load data points were converted as stress values and plotted in the S-N curve. By using equation 1 stress range can be predicted and equation 2 gave values for stress amplitude. Similarly, Equations 3-5 can be used to find the mean stress, stress

ratio, and amplitude, respectively. Stress amplitudes and life cycles were plotted (in log scale on the X-axis). In fig 4, all four post-processing conditions of X-direction printed samples are plotted. For the various condition, the same load (490 MPa) different S-N curves were observed, however considerable scatter was evident. Importantly, it was observed that machining improved the fatigue strength significantly. S-N curves were shifted above the printed samples' fatigue value. The rough surface of printed samples likely lowered fatigue life compared to the smoother after machining. Around 10 million cycles' fatigue value is significantly improved for condition B. Also, machining followed by micro shot-peening was recommended in the literature [21] for improved fatigue strength because it improves the compressive residual stress and closes the pores over the surface.
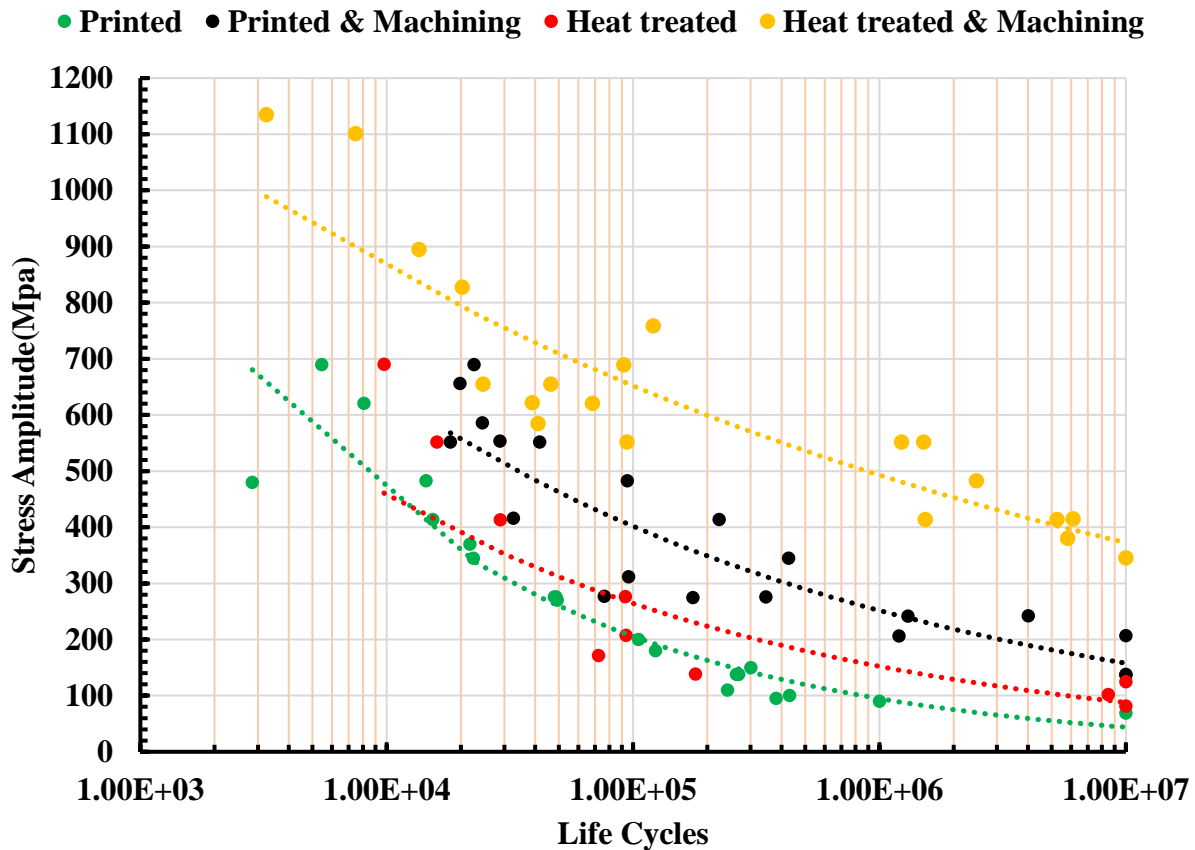

Figure 5 S-N curves for the samples printed in the Z direction.

Similarly, heat-treated X-direction printed samples had improved fatigue strength but were not high as machining. During aging, material strength increased (approximately doubles compared to as printed) and residual stresses were relieved. However, aging reduces ductility which likely reduces fatigue life. When machining and heat treatment processes were combined, fatigue strengths improved significantly because heat treatment increased strength and machining improve the surface finish.

Z-direction printed samples exhibited lower fatigue strength compared to X-direction printed samples for all post-processing conditions. The main reason for the lower fatigue life was the anisotropy inherent in the layer-wise PBF process. So, based on the results, build directions

have a significant role to play in the fatigue strength. Other than that, Z-direction printed samples followed the same trends and can be observed in fig 5. Similar to X-direction S-N curves, machining played a significant role in improving fatigue life. Heat-treatment alone had a modest effect, but heat-treatment and further machining improved the fatigue life significantly.

Despite the scatter of AM results in the S-N curve, it was observed that build orientation has a significant role in the fatigue behavior of the maraging steels. Similarly, each post-processing condition influenced the fatigue strength of the material. Especially, machining and heat treatment combined with machining played a significant role in both X and Z directions.

Conclusion

This research study investigated the fatigue strength of maraging steel manufactured by an EOS M280 PBF machine for different post-processing conditions such as as-printed(A), printed and machined(B), heat-treated(C), and heat-treated and machined(D) along with X and Z built orientations. A characterization method for additive manufactured materials was used to select the sample count and select equivalent test methods for fatigue tests. S-N curves were developed for tests conducted using the HCF regime. The findings of the research study are summarized below.

1. X-direction printed samples without any post-processing provided better fatigue strength than Z-direction printed samples. The main reason was the anisotropy inherent in the PBF process. Therefore, the build orientation influenced the fatigue life of the samples.
2. Surface defects and high surface roughness were reduced by machining, which improved fatigue strength and life significantly.
3. Aging heat treatment improved the fatigue life but not as significantly as machining.
4. Aging and machining resulted in significantly improved fatigue strength, compared to the as-printed condition. This combination resulted in the highest fatigue strengths and lives and should be recommended for in applications.

Acknowledgment

References

[1]   Ian Gibson; David Rosen; Brent Stucker; Mahyar Khorasani, *Additive Manufacturing Technologies*, 3rd edition. Springer, 2021.
[2]   J. Suryawanshi, K. G. Prashanth, and U. Ramamurty, "Tensile, fracture, and fatigue crack growth properties of a 3D printed maraging steel through selective laser melting," *J. Alloys Compd.*, vol. 725, pp. 355–364, 2017, doi: 10.1016/j.jallcom.2017.07.177.
[3]   Z. Zhang, M. Koyama, M. M. Wang, K. Tsuzaki, C. C. Tasan, and H. Noguchi, "Microstructural mechanisms of fatigue crack non-propagation in TRIP-maraging steels," *Int. J. Fatigue*, vol. 113, no. April, pp. 126–136, 2018, doi: 10.1016/j.ijfatigue.2018.04.013.

[4]   N. E.Dowling, *Mechanical Behaviour of Materials*, Fourth. 2013.

[5]   D. Croccolo, M. De Agostinis, S. Fini, G. Olmi, A. Vranic, and S. Ciric-Kostic, "Influence of the build orientation on the fatigue strength of EOS maraging steel produced by additive metal machine," *Fatigue Fract. Eng. Mater. Struct.*, vol. 39, no. 5, pp. 637–647, 2016, doi: 10.1111/ffe.12395.

[6]   N. Croccolo, Dario; De Agostinis, Massimiliano; Fini, Stefano; Olmi, Giorgio; Robusto, Francesco; Ćirić-Kostić, Snežana;Morača, Slobodan; Bogojević, "Sensitivity of direct metal laser sintering Maraging steel fatigue strength to build orientation and allowance for machining," *Fatigue Fract. Eng. Mater. Struct.*, vol. 42, no. 1, pp. 374–386, 2019, doi: 10.1111/ffe.12917.

[7]   Z. F. . Wang, B.; Zhang, P.; Duan, Q. Q.; Zhang, Z. J.; Yang, H. J.; Li, X. W.; Zhang, "Optimizing the fatigue strength of 18Ni maraging steel through ageing treatment," *Mater. Sci. Eng. A*, vol. 707, no. August, pp. 674–688, 2017, doi: 10.1016/j.msea.2017.09.107.

[8]   N. Kawagoishi, T. Nagano, M. Moriyama, and E. Kondo, "Improvement of fatigue strength of maraging steel by shot peening," *Mater. Manuf. Process.*, vol. 24, no. 12, pp. 1431–1435, 2009, doi: 10.1080/10426910903386055.

[9]   N. Kawagoishi, K. Morino, H. Nisitani, N. Yan, and T. Yamakita, "Fatigue strength of nitrided 18Ni 300 grade maraging steel," *Key Eng. Mater.*, vol. 251–252, pp. 33–40, 2003, doi: 10.4028/www.scientific.net/kem.251-252.33.

[10]   H. Fitzka, Michael; Pennings, Bert; Karr, Ulrike; Schönbauer, B.; Schuller, Reinhard; Tran, Minh Duc; Mayer, "Influence of cycling frequency and testing volume on the VHCF properties of 18Ni maraging steel," *Eng. Fract. Mech.*, vol. 216, no. June, p. 106525, 2019, doi: 10.1016/j.engfracmech.2019.106525.

[11]   H. Karr, Ulrike; Schuller, Reinhard; Fitzka, Michael; Schönbauer, Bernd; Tran, Duc; Pennings, Bert; Mayer, "Influence of inclusion type on the very high cycle fatigue properties of 18Ni maraging steel," *J. Mater. Sci.*, vol. 52, no. 10, pp. 5954–5967, 2017, doi: 10.1007/s10853-017-0831-1.

[12]   A. Liu, Chao; Zhao, Ming Chun; Zhao, Ying Chao; Zhang, Le; Yin, Deng Feng; Tian, Yan; Shan, Yi Yin; Yang, Ke; Atrens, "Ultra-high cycle fatigue behavior of a novel 1.9 GPa grade super-high-strength maraging stainless steel," *Mater. Sci. Eng. A*, vol. 755, no. April, pp. 50–56, 2019, doi: 10.1016/j.msea.2019.03.120.

[13]   G. Meneghetti, D. Rigon, D. Cozzi, W. Waldhauser, and M. Dabalà, "Influence of build orientation on static and axial fatigue properties of maraging steel specimens produced by additive manufacturing," *Procedia Struct. Integr.*, vol. 7, pp. 149–157, 2017, doi: 10.1016/j.prostr.2017.11.072.

[14]   G. Meneghetti, D. Rigon, and C. Gennari, "An analysis of defects influence on axial fatigue strength of maraging steel specimens produced by additive manufacturing," *Int. J. Fatigue*, vol. 118, no. August 2018, pp. 54–64, 2019, doi: 10.1016/j.ijfatigue.2018.08.034.

[15]   J. Antunes, Fernando; Santos, Luís; Capela, Carlos; Ferreira, José; Costa, José; Jesus and P. Prates, "Fatigue crack growth in maraging steel obtained by Selective Laser Melting," *Appl. Sci.*, vol. 9, no. 20, pp. 1–13, 2019, doi: 10.3390/app9204412.

[16]   J. M. Santos, L. M.S.;Ferreira, J. A.M.;Jesus, J. S.;Costa and C. . Capela, "Fatigue behaviour of selective laser melting steel components," *Theor. Appl. Fract. Mech.*, vol. 85, pp. 9–15, 2016, doi: 10.1016/j.tafmec.2016.08.011.

[17]   N. Raju, S. Kim, and D. W. Rosen, "A characterization method for mechanical properties of metal powder bed fusion parts," *Int. J. Adv. Manuf. Technol.*, vol. 108, no. 4, pp. 1189–

1201, 2020, doi: 10.1007/s00170-020-05298-7.

[18] ASTM International, "ASTM E 122 - 07 Standard Practice for Calculating Sample Size to Estimate , With Specified Precision , the Average for a Characteristic of a Lot or," 2009. doi: 10.1520/E0122-17.2.

[19] Slotwinski, John; Moylan, "Applicability of existing materials testing standards for additive manufacturing materials," 2015, doi: http://dx.doi.org/10.6028/NIST.IR.8005.

[20] EOS, "Parameter sheet Machine and software parameters EOSINT M 280 Parameter sheet Parameter sets – Hardware settings," 2014.

[21] N. Croccolo, Dario; De Agostinis, Massimiliano; Fini, Stefano; Olmi, Giorgio; Robusto, Francesco; Kostić, Snežana Ćirić; Vranić, Aleksandar; Bogojević, "Fatigue response of as-built DMLS maraging steel and effects of aging, machining, and peening treatments," *Metals (Basel).*, vol. 8, no. 7, 2018, doi: 10.3390/met8070505.